Phase diagram study and thermodynamic modeling of the $CaO-TiO_2-CaF_2$ system

Jiho Bang[1], *In-Ho Jung*[1,*]

1. Department of Materials Science and Engineering, Seoul National University, Seoul, South Korea, 08826. email: lpiok@snu.ac.kr
* Department of Materials Science and Engineering, Seoul National University, Seoul, South Korea, 08826. email: in-ho.jung@snu.ac.kr

Keywords: Phase diagram, $CaO-TiO_2-CaF_2$ system, Thermodynamic database, ESR slag

ABSTRACT

Ti is an important constituent for steels and superalloys. During the continuous casting process and ElectroSlag Remelting process (ESR), Ti in molten steel and superalloy can have chemical reactions with casting flux and ESR slag containing CaO and CaF_2. In order to investigate such exchange reactions, the understanding of the (Ca,Ti//O,F) reciprocal slag system is prerequisite. In the present study, a coupled phase diagram experiment and thermodynamic modeling of the (Ca,Ti//O,F) reciprocal system was performed. In particular, the phase diagram of the CaF_2-TiO_2 system was experimentally investigated by Differential Thermal Analysis (DTA) experiment, and quenching experiments followed by Electron Probe MicroAnalysis (EPMA) phase analysis. The Gibbs energy functions of all solid and liquid phases in the (Ca,Ti//O,F) reciprocal system were optimized to reproduce the present data and all available reliable experimental data in literature.

INTRODUCTION

ElectroSlag Remelting(ESR) process is widely used in the refining process of superalloy and special steel due to its superior advantages such as homogenization, desulfurization, non-metallic inclusion removal and macro/micro-segregation control in alloy products (Arh, Podgornik and Bojan, 2016; Shi, Zhang et al., 2021). However, chemical reaction between liquid metal and slag can take place during ESR process, which induces the change in alloy composition in liquid metal (Chen, Wang and Hu, 2013). In particular, the content of strong oxidizing element such as Ti, Al, and Si can be readily varied by the reaction with ESR slag. Therefore, the understanding of the chemical reaction between liquid metal and ESR slag is important for accurate control of final target product composition in ESR process. Previous studies (Hou et al., 2016; Hou et al., 2018; Jiang et al., 2016; Pateisky, Biele, and Fleischer, 1972) on the equilibration between slag and molten metal showed that the chemical composition of ESR slag and remelting condition influence the final liquid metal composition significantly.

Conventional ESR slag is composed of CaO, CaF_2 and Al_2O_3. In order to understand the distribution of Ti between liquid metal and ESR slag, the understanding of $CaO-CaF_2-Al_2O_3-TiO_2$ slag system is essential. Jung and his colleague (Jung et al. 2015) performed the thermodynamic modeling of the oxyfluoride system $CaO-MgO-Al_2O_3-SiO_2-Na_2O-K_2O-Li_2O-ZrO_2-F$, which is already available in FactSage FTOxid database (Bale et al., 2016). However, the system containing Ti oxide has not been assessed well for oxyfluoride system. Experimentally the $CaF_2-CaO-TiO_2$ system has not been well investigated yet.

The purpose of this study is to investigate the phase diagram of the $CaF_2-CaO-TiO_2$ system and develop a thermodynamic database for the system. Due to the high vapor pressure of CaF_2 and strong reactivity of CaO-containing slag, the phase diagram experiment was conducted using sealed Pt crucible. Based on the phase diagram data in this study, the thermodynamic modeling of the $CaF_2-CaO-TiO_2$ system was performed using the Calculation of the PHAse Diagram (CALPHAD)

method. All thermodynamic calculations were conducted using FactSage thermochemical software (Bale et al., 2016).

LITERATURE REVIEW

Thermodynamic assessments of binary CaF_2-CaO (Kim et al., 2012), and CaO-TiO_2 (Du and Jung, 2023) have been well-conducted. The phase diagram of the CaF_2-CaO-TiO_2 system was previously investigated by Hillert (Hillert, 1965a and 1965b). He conducted equilibrium experiments on the CaF_2-TiO_2 and CaF_2-CaO-TiO_2 system using the quenching method. The microstructures of samples were analysed using optical microscopy and X-Ray diffraction (XRD) method. The phase diagram of the CaF_2-TiO_2 reported by Hillert is presented in Fig. 1. Hillert presented the existence of liquid miscibility gap between 0.46 ~ 0.94 CaF_2 mol fraction and reported an eutectic reaction of L → TiO_2 + CaF_2 at 0.42 CaF_2 and 1360 °C. However, because the experiments were conducted using open Pt crucibles, the composition of initial samples could be changed due to the possible evaporation of CaF_2. In addition, there would be a high chance of quenched crystals formation during quenching process, which would mislead the interpretation of the results.

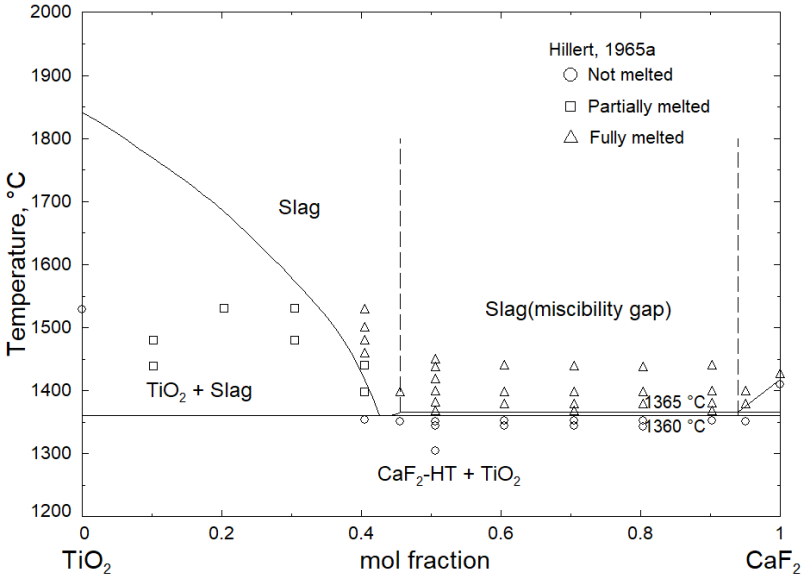

FIG. 1 – Phase diagram of the CaF_2-TiO_2 system reported by Hillert (redrawn from original diagram by Hillert, 1965a).

PHASE DIAGRAM EXPERINMETS

- Experimental challenges

There were three major challenges in conducting the phase diagram experiment of the CaF_2-CaO-TiO_2 system: (i) high vapor pressure of CaF_2 and gas reactivity of CaO-rich slag, (ii) difficulty in oxyfluoride sample composition analysis using electron probe micro-analyzer (EPMA) and (iii) formation of quenched crystals due to low viscosity of CaF_2-containing melt. These experimental challenges were resolved by employing sealed Pt crucible, and oxyfluoride standard in EPMA analysis. Unfortunately, quenched crystal formation cannot be avoided. In order to resolve difficulty in EPMA composition analysis due to quenched crystal formation, a large beam size of 10~30 μm was employed in the analysis to measure overall composition of original liquid phase. Potential sample damage due to evaporation of F in EPMA was minimized by employing a low voltage and amperage condition, 10 kV and 10 nA.

- Starting materials

The mixtures of pure CaF_2 (Sigma-aldrich; 99.99 wt.% purity), TiO_2 (Sigma-aldrich; 99.9 wt.% purity) powders were prepared for the starting materials. To prevent hydration of starting samples, each powder was dried separately at high temperature before preparing the mixtures: drying of CaF_2 at 800 °C, and TiO_2 at 1200 °C for 1day. Dried powders were stored in vacuum desiccator to prevent

moisture pickup. Starting samples were prepared by mixing dried powders using an alumina mortar with C_6H_{12}-cyclohexane to prevent moisture pickup. In order to confirm no oxidation of CaF_2 powder to CaO before sample preparation, XRD analysis was conducted and no CaO peaks were detected. To prevent vaporization of CaF_2 during equilibration experiment and hydration during quenching process, samples were put in sealed in Pt crucibles (4 mm in outer diameter, 3 mm inner diameter, and 10 mm length). The leakage of the sealed crucibles was checked by sonicating the crucibles in water for 10 minutes and monitoring mass changes before and after sonication.

- Differential Thermal Analysis (DTA) experiments

DTA experiment was conducted using the Netsch STA 449 F5 equipment. Temperature calibration on DTA was performed using phase transition temperatures of Ag_2SO_4, $BaCO_3$, $C_7H_6O_2$, $C_{12}H_{10}$, CsCl, $CaMgSi_2O_6$, K_2CrO_4, $KClO_4$, and $RbNO_3$. Experiment was conducted with a sealed Pt crucible directly placed into DTA alumina crucible. To minimize the effect of Pt crucible in the analysis, a reference was taken with empty Pt crucible and DTA alumina crucible.

Sample with $0.5CaF_2$-$0.5TiO_2$ in mol fraction was used for DTA experiments. Sample was heated and cooled at a rate of 10 K/min up to 1400 °C under an Ar gas with 20 ml/min flowrate. Possible leakage of Pt crucible was continuously monitored using simultaneous thermogravity analysis in DTA equipment, and weight change of Pt crucible before and after experiment was also checked to confirm no vaporization loss of CaF_2.

- Quenching experiments

Equilibration and quenching experiments were performed in a vertical tube furnace. Temperature of the furnace was measured by using a B-type thermocouple and maintained within 3 °C range of the target temperature using PID controller. Sealed Pt crucibles were hanged in the hot zone (1200~1400 °C) of the vertical furnace for equilibrium for 2~3 hr using Pt wire. After equilibration, samples were quenched by dropping into cold water. Possible leakage of the sample during experiment was checked by measuring the mass change of sealed Pt crucibles before and after the experiments. Due to high vapor pressure of the CaF_2-containing slag, ordinary Pt crucibles (3.3 mm outer diameter, 3 mm inner diameter, and 10 mm length) were broken during long equilibration experiments at high temperature. Therefore, thick Pt crucibles (4 mm in outer diameter, 3 mm inner diameter, and 10 mm length) were used in this experiment.

- Phase analysis

After quenching experiments, sample were examined by XRD analysis (Bruker D8 Advance) and EPMA (JEOL-8530F). For XRD analysis, the samples were grounded and examined using Cu-Kα source (λ = 1.54 Å). Measured peaks were compared with powder diffraction files (PDF) of Bruker AXS DIFFRAC.EVA software. For EPMA, samples were mounted using epoxy and polished longitudinally using SiC paper of 400, 800, 1200, 2000 grit and diamond based oil. Oil based polishing was conducted to exclude moisture pickup. After polishing, sonication using cyclohexane-C_6H_{12} was conducted and carbon coating was conducted. For EPMA, accelerating voltage of 10 kV and beam current of 10 nA was implemented. As finely distributed quenched crystals were inevitably formed in liquid region of quenched sample, a large beam size of 10~30 μm was used to obtain the overall liquid composition by averaging fluctuations in the sample composition caused by quenched crystals.

As the present samples have oxyfluoride chemistry, both mass balance and charge balance should be accomplished to determine the exact composition of the samples. However, when calibrating raw data using PRZ Armstrong algorithm with oxide and CaF_2 as standards, charge balance of the sample could not be easily accomplished. Therefore, a quenched liquid sample of 0.7 CaF_2-0.3 TiO_2 mol fraction was intentionally prepared from 1400 °C and used for internal standard of EPMA for Ca, Ti, O, and F concentration. It should be noted that very fine and homogenous quenched crystals of CaF_2 and TiO_2 were dispersed in the reference standard sample, as shown in Fig. 2.

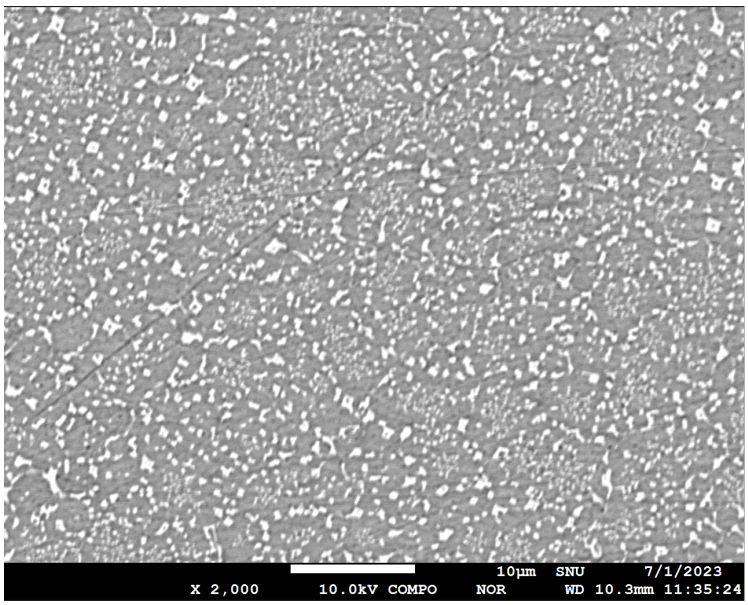

FIG. 2 – Microstructure of the EPMA standard sample (0.7 CaF_2-0.3 TiO_2 in mol fraction) quenched at 1400 °C. White crystals and dark crystals are TiO_2 and CaF_2, respectively.

THERMODYNAMIC MODEL

The Gibbs energy of pure elements and stoichiometric compounds can be expressed by heat capacity(Cp), and standard enthalpy of formation (ΔH^o_{298K}) and standard entropy (S^o_{298K}) at 298.15 K as following Eq.(1).

$$G^o_T = \Delta H^o_{298K} + \int_{298}^{T} C_{p,T}\,dT - T\left(S^o_{298K} + \int_{298}^{T} \frac{C_{p,T}}{T}\,dT\right) \qquad \text{Eq.(1)}$$

The Gibbs energy of liquid oxyfluoride solution was described by using Modified Quasichemical Model(MQM) (Pelton et al., 2000; Pelton and Chartrand, 2001) which considers the Short Range Ordering(SRO) of the nearest-neighbor atoms. The advantages of MQM compared with Bragg-Williams Random Mixing Model (BRWMM) are (i) the automatic change of non-ideal mixing entropy of solution depending on ordering tendency by interaction between solution species, (ii) freedom to modify the coordination number of component to reproduce SRO in binary liquid solution depending on system by system, and (iii) flexible choice of ternary interpolation technique depending on thermodynamic behaviour of each ternary system.

For oxide system, SRO between cations with a common oxygen anion is considered. However, as CaF_2-CaO-TiO_2 system is a reciprocal (Ca,Ti//O,F) system with two cations and two anions, two sublattice quadruplet approximation was implemented on MQM to consider first-nearest neighbour and second nearest neighbour SRO simultaneously (Chartrand, and Pelton, 2001; Pelton, Chartrand and Eriksson, 2001). In the (Ca,Ti//O,F) reciprocal system, Ca^{2+} and Ti^{4+} are considered to be located in imaginary cationic sublattice and O^{2-} and F^- are considered to be located in imaginary anionic sublattice in the melt, as shown in Fig. 3. The SRO of Ca^{2+} and Ti^{4+} cations can be expressed by binary interaction term of $\Delta g_{CaTi/OO}$ or $\Delta_{gCaTi/FF}$ which could be optimized for CaO-TiO_2 melt and CaF_2-TiF_4 melt, respectively. Similarly, binary model parameters of $\Delta g_{Ca/OF}$ and $\Delta g_{Ti/OF}$ can be optimized for binary CaO-CaF_2 and TiO_2-TiF_4, respectively. Reciprocal interaction parameters of $\Delta g_{CaTi/OF}$ and ternary interaction parameters can be also added to optimize the Gibbs energy of reciprocal melt.

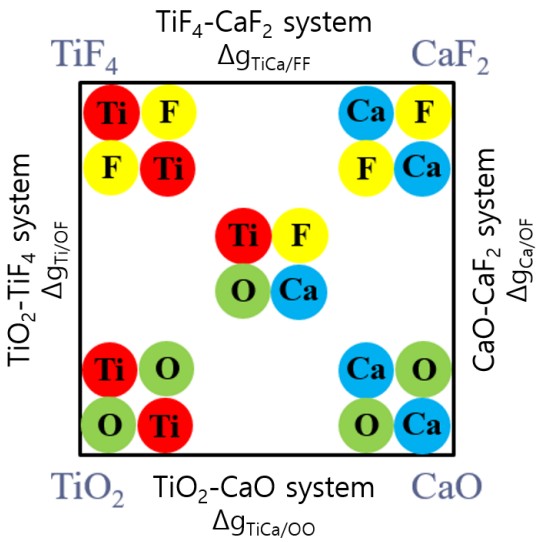

FIG. 3 – Schematic diagram of two sublattice approximation of (Ca,Ti//O,F) reciprocal system. $Ca^{2+}$and Ti^{4+} located in cation sublattices and O^{2-} and F^{-} located in anion sublattices.

EXPERIMENTAL RESULTS AND THERMODYNAMIC MODELING

- Experimental results

The phase diagram of the CaF_2-TiO_2 system based on the present experimental data and thermodynamic modelling results is presented in Fig. 4.

The DTA results for $0.5CaF_2$-$0.5TiO_2$ sample is presented in Fig. 4 (a). As shown in the DTA curves for all 3 cycles, the transition peaks for the sample were not very discrete enough to ensure a clear phase transformation. Other DTA results for CaF_2-containing samples showed similar trend. Based on the heating curve data, the onset temperature for the phase transition was identified at 1349.5 °C. The transition temperature in cooling curves was also the same as the value from heating curves.

In order to clearly determine the transition occurring at this transition temperature, quenching experiments at 1250 and 1400 °C were conducted for the same samples and the BSE images of the quenched samples are presented in Fig. 4 (b) and (c), respectively. Based on both XRD and EPMA results, the equilibrium phases at 1250 °C and 1400 °C were determined to be CaF_2 + TiO_2, and TiO_2 + Liquid, respectively. EPMA results indicate that no mutual solubility between CaF_2 and TiO_2 in solid state. The liquidus of TiO_2 at 1400 °C was determined to be $0.7CaF_2$-$0.3TiO_2$. In order to confirm the liquidus of this system, a sample of $0.8CaF_2$-$0.2TiO_2$ was prepared and equilibrated at 1400 °C. The resultant phase confirmed no solid TiO_2 formation.

- Thermodynamic modeling

For thermodynamic modeling, the Gibbs energies of solid phases were taken from constituent binary system of the CaO-TiO_2 and CaF_2-CaO in FactSage FTOxide 8.3 database. No ternary or reciprocal solids were found in the (Ca,Ti // O,F) reciprocal system. To reproduce the phase diagram data in this study for the entire of (Ca,Ti // O,F) reciprocal system including the phase diagram information in Fig. 4 and other pseudo-binary and isopleth sections (not presented here), reciprocal MQM parameters were optimized.

The calculated phase diagram from optimized model parameters is in good agreement with experimental data in this study, as shown in Fig. 4. Several points are need to be highlighted regarding the differences between the previous experimental results (Hillert, 1965a) and this optimized phase diagram. First, the miscibility gap reported in previous study was not substantiated in this study because a miscibility gap could not be observed in this experiment. As the previous study analysed sample using optical microscopy and XRD, the quenched crystals of CaF_2 and TiO_2 shown in Fig. 2 could be misunderstood as a liquid immiscibility. Second, several experimental points reported as partially melted region were found to be a liquid single phase region in the present phase diagram study. Considering the high vapor pressure of CaF_2, sample composition of the previous

study with open crucible might be shifted toward TiO_2-rich composition, which induces this misinterpretation. Finally, considerable number of experimental data reported single phase at the range of 0.46CaF_2 to 0.80CaF_2 in mol fraction at 1365 °C, 1380 °C and 1400 °C. However, in the present experiment, Liquid + TiO_2 phase assemblage is found in the 0.5CaF_2 mol fraction sample at 1400 °C. We found that solid TiO_2 crystals settled down on the bottom of the sample and leave liquid phase in the upper side. This seems to happen because of very low viscosity of CaF_2 containing slag. This kind of settling of solid TiO_2 crystal in a large sample size might lead to the wrong interpretation of the equilibrium results in the previous study by Hillert (1965a). Solid crystal settlement was also observed in other experiments (unpublished results by the present authors) for oxyfluoride systems containing CaF_2.

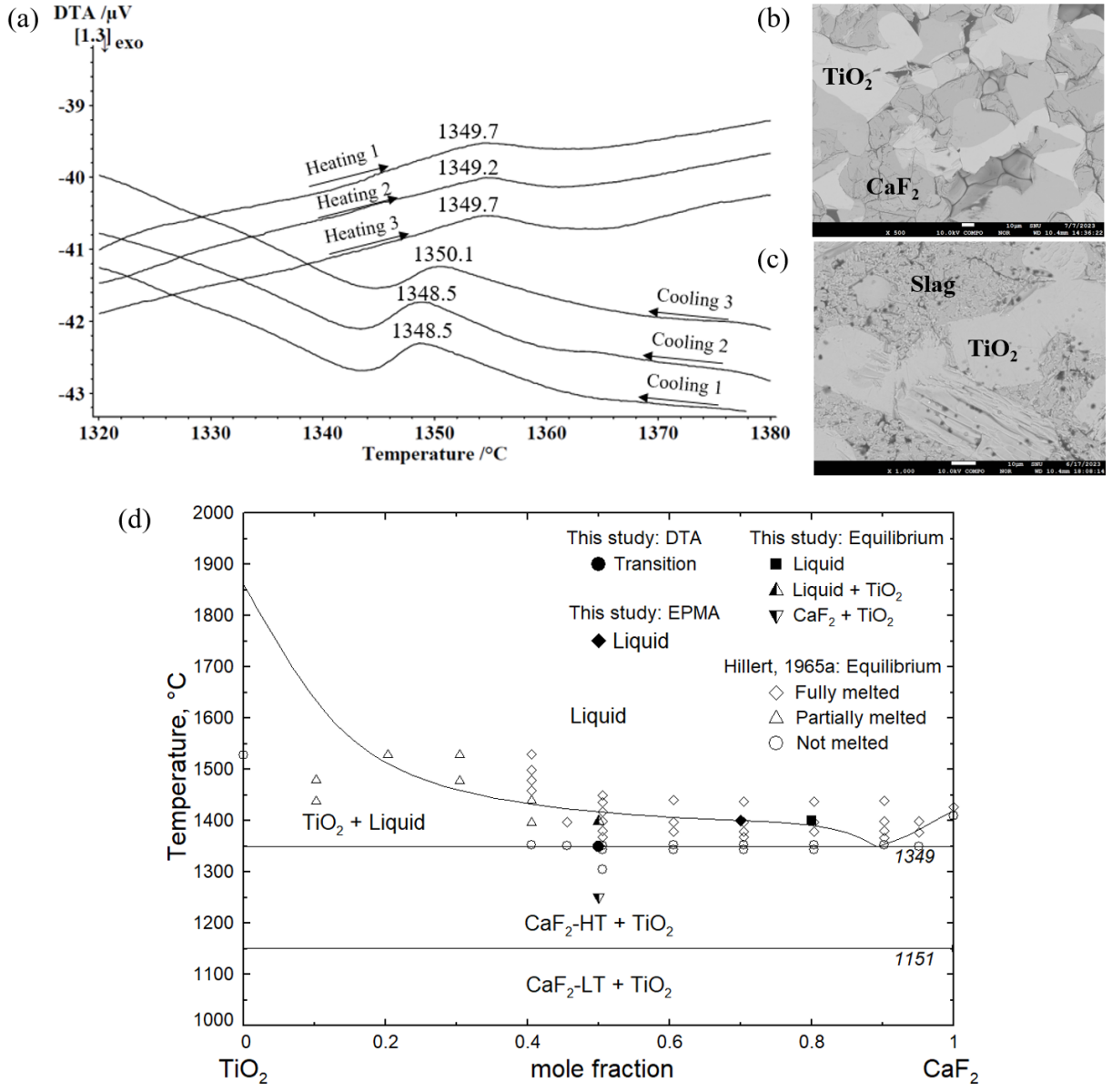

FIG. 4 – Phase diagram of the CaF_2-TiO_2 system optimized in this study. (a) DTA result, and BSE images of sample equilibrated at (b) 1250 °C and (c) 1400 °C with starting composition of 0.5CaF_2 - 0.5 TiO_2. (d) Optimized phase diagram based on the present experimental data along with previous experimental results by Hillert (1965a).

CONCLUSIONS

The phase diagram of the CaF_2-TiO_2 system was experimentally determined using DTA and quenching experiments followed by EPMA and XRD phase analysis. Sealed Pt crucible was employed for the experiment to overcome experimental challenges in oxyfluoride system. It is found

that the previously reported phase diagram of the CaF_2-TiO_2 system is inaccurate. More reliable phase diagram of the CaF_2-TiO_2 system was constructed from the present coupled phase diagram experiment and thermodynamic modeling study. The resultant thermodynamic database can be integrated to the existing FactSage database to calculate the multicomponent phase diagram for oxyfluoride slag system containing TiO_2 and also for slag-metal equilibrium calculation for continuous casting steel process and ESR process.

ACKNOWLEDGEMENTS

This research was supported by Manufacturing and Evaluation Technology of Premium Quality Inconel 718 Alloy Ingot and Forging Product for Turbofan Rotor Disk funded by Ministry of Trade, Industry and Energy (No. RS-2023-00256058). Financial supports from Tata Steel Europe, Posco, Hyundai Steel, Nucor Steel, RioTionto Iron and Titanium, Nippon Steel Corp., JFE Steel, Voestalpine, RHI Magnesita, SeAH Besteel, Doosan Heavy Industry and Construction, and SCHOTT AG are also gratefully acknowledged.

REFERENCES

Arh, B, Podgornik, B, and Burja, J, 2016. Electroslag remelting: A process overview, *Mater. Technol*, 50(6):971-979.

Bale, C W, Bélisle, E, Chartrand, P, Decterov, S A, Eriksson, G, Gheribi, A E and Van Ende, M A, 2016. Reprint of: FactSage thermochemical software and databases, 2010–2016. *Calphad*, 55:1-19.

Chen, C Y, Wang, G and Hu, Y, 2013. Composition variation in Incoloy 800H alloy ingot during ESR process, *China Steel Technical Report*, 26:7-12.

Du, G and Jung, I H, 2023. Unpublished report

Shi, C B, Huang, Y, Zhang, J X, Li, J and Zheng, X, 2021. Review on desulfurization in electroslag remelting, *International Journal of Minerals, Metallurgy and Materials*, 28:18-29

Hillert, M, 2001. The compound energy formalism, *Journal of Alloys and Compounds*, 320(2):161-176.

Hillert, L, 1965a. Phase Diagram TiO_2-CaF_2, *Acta Chemica Scandinavica*, 19(6):1516.

Hillert, L, Bo, H, Magnéli, A, and Kallner, A, 1965b. The phase diagram (81% TiO_2+ 19% CaO)-CaF_2, *Acta Chemica. Scand*, 19:1986-1987.

Hou, D, Liu, F B, Qu, T P, Jiang, Z H, Wang, D Y and Dong, Y W, 2018. Behavior of alloying elements during drawing-ingot-type electroslag remelting of stainless steel containing titanium, *ISIJ International*, 58(5):876-885.

Hou, D, Jiang, Z, Dong, Y, Cao, Y, Cao, H and Gong, W, 2016. Thermodynamic design of electroslag remelting slag for high titanium and low aluminium stainless steel based on IMCT, *Ironmaking & Steelmaking*, 43(7):517-525.

Jiang, Z H, Hou, D, Dong, Y W, Cao, Y L, Cao, H B and Gong, W, 2016. Effect of slag on titanium, silicon, and aluminum contents in superalloy during electroslag remelting, *Metallurgical and Materials Transactions B*, 47:1465-1474.

Jung, I-H, Van Ende M-A, Kim D.-G., Konar B, Kwon S.-Y, 2015. Thermodynamic database for oxy-fluoride mold flux, CaO-MgO-Na2O-K2O-Li2O-Al2O3-SiO2-ZrO2-F, *Asia Steel 2015*: 476-477

Kim, D G, van Hoek, C, Liebske, C, van der Laan, S, Hudon, P and Jung, I H, 2012. Phase Diagram Study of the CaO–CaF_2 System, *ISIJ international*, 52(11):1945-1950.

Pateisky, G, Biele, H and Fleischer, H J, 1972. The reactions of titanium and silicon with Al_2O_3-CaO-CaF_2 slags in the ESR process, *Journal of Vacuum Science and Technology*, 9(6):1318-1321.

Pelton, A D, Degterov, S A, Eriksson, G, Robelin, C and Dessureault, Y, 2000. The modified quasichemical model I—Binary solutions, *Metallurgical and Materials Transactions B*, 31:651-659.

Pelton, A D and Chartrand, P, 2001. The modified quasi-chemical model: Part II. Multicomponent solutions, *Metallurgical and Materials Transactions A*, 32:1355-1360.

Chartrand, P and Pelton, A D, 2001. The modified quasi-chemical model: Part III. Two sublattices, *Metallurgical and Materials Transactions A*, 32:1397-1407.

Pelton, A. D, Chartrand, P and Eriksson, G, 2001. The modified quasi-chemical model: Part IV. Two-sublattice quadruplet approximation, *Metallurgical and Materials Transactions A*, 32:1409-1416.